



PSEUDOLITE AUGMENTATION FOR GNSS-BASED MONITORING OF LARGE ENGINEERING STRUCTURES

Luis SERRANO, Charles DIXON, and Reinhard HAAS

Future Navigation Applications, EADS Astrium UK Ltd.

Abstract: The demand for real-time high accuracy and reliable positioning has been continuously increasing, and in particular, GNSS-based monitoring stresses requirements on continuous positioning with higher reliability. Unfortunately, blockages (natural and man-made), causing shadowing and multipath represent an adverse condition for Global Navigation Satellite System (GNSS) signal reception, thus leading to poor satellite visibility and low positioning accuracy in many dam deformation monitoring scenarios.

Pseudolites (Pseudo-Satellites), which fit into the category of ground-based augmentation systems (GBAS) that transmit GNSS-like signals, can improve the transmitter-receiver geometry and can be used as additional range observations to improve the performance of a purely GNSS-based deformation monitoring system. However, due to cost reasons and environment constraints, the number of pseudolites that can be installed must be assessed.

This paper demonstrates a simulation study by EADS Astrium for evaluating the technical appropriateness of installing pseudolites as an augmentation system. The simulation relies on precise GNSS-satellite orbital information, digital elevation model, pseudolite transmitter location and respective signal propagation characteristics. All the information was integrated with a 3-D model of a dam structure in order to obtain a realistic and reliable simulation.

1. INTRODUCTION

Pseudolites have been used to augment the GNSS constellation or to form an independent system for positioning and navigation. The intention of EADS Astrium, as an industrial provider of GNSS/pseudolite systems, is to perform investigations in this area with a special emphasis on tackling some of its known problems. Even though EADS Astrium has been employing this system thus far for pseudorange-based applications it is foreseeable that its use can be extended to GNSS-based monitoring systems (hence with carrier-phase observations).

In this paper we cover the technicalities and specifications of EADS Astrium pseudolite-infrastructure, and we briefly overview known pseudolite signal errors. Then, based on the aforementioned typical errors we demonstrate how our team performs feasibility studies to assess improvements in terms of accuracy and continuity when using pseudolite augmentation. Using a well known engineering structure, the Hoover dam, we demonstrate how a pseudolite augmentation system can effectively increase the accuracy and continuity of estimated deformation monitoring control points.

2. EADS ASTRIUM PSEUDOLITE SYSTEM

Similar to the GPS programme in its initial inception, the new global navigation satellite system Galileo under development by the European Union also used the pseudolite concept to test and validate frequency allocation and user equipment. EADS Astrium has been deeply involved in that stage and the Astrium pseudolite system currently being developed / commercialized evolved from there. For more details we refer to the website <http://gnss-technology.com>, where one can see a thorough description of the pseudolite system specifications. The central part of this system is the GNSS ranging-signal generator which is depicted in the next figure:



Figure 1 - EADS Astrium NSG 5100 GNSS-like Signal Generator

The specifications regarding the output signals, and their respective frequencies, are described in next table:

Table 1 - NSG 5100 Signal generator output, and frequency signals

Output Signals	Frequencies (switchable)
<i>E5 (E5a/ E5b)</i>	1191.795 MHz
<i>L1</i>	11575.42 MHz
<i>E6</i>	1278.75 MHz
Doppler Range	±10 KHz in steps of 1 mHz

In figure 2 one can see an example of EADS Astrium pseudolite's operation concepts. The transmit signal stations are easily deployable for most applications and are provided with a weather-proof enclosure. For more information please refer to the MARUSE project.

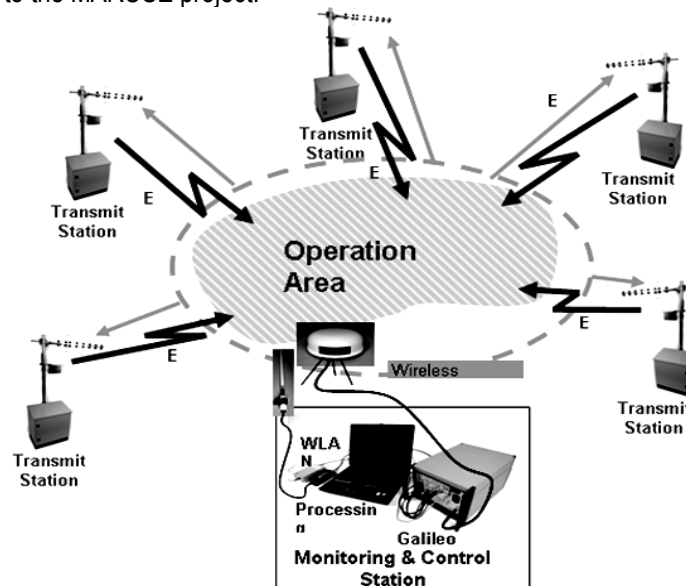


Figure 2 - EADS Astrium pseudolites operation concept (taken from the GSA MARUSE project)

3. PSEUDOLITE -GNSS / RTK AUGMENTATION SYSTEM

The EADS Astrium pseudolite system works as a ground-based GNSS-like signal augmentation system and thus we assume that any brand of GNSS-RTK receivers and respective processing software can be used with Astrium's pseudolite signals. We use in this paper a 3-D model of the Hoover dam (figure 3) for simulation



purposes. The Hoover dam is not only a huge and complex engineering structure but it is also implanted in a river gorge thus making a perfect simulation example for a scenario of poor GNSS signal visibility.



Figure 3 - Hoover dam

For certain reference monitoring points on the dam structure there are many periods where the number of visible satellites is not sufficient to obtain a 3D solution. However, two pseudolites positioned at both sides of the dam (figure 4) augmenting the satellite coverage and adding up to five ranging signals should allow a RTK fixed-solution for typical high-end dual-frequency receivers, and for a short-distance GNSS reference station.

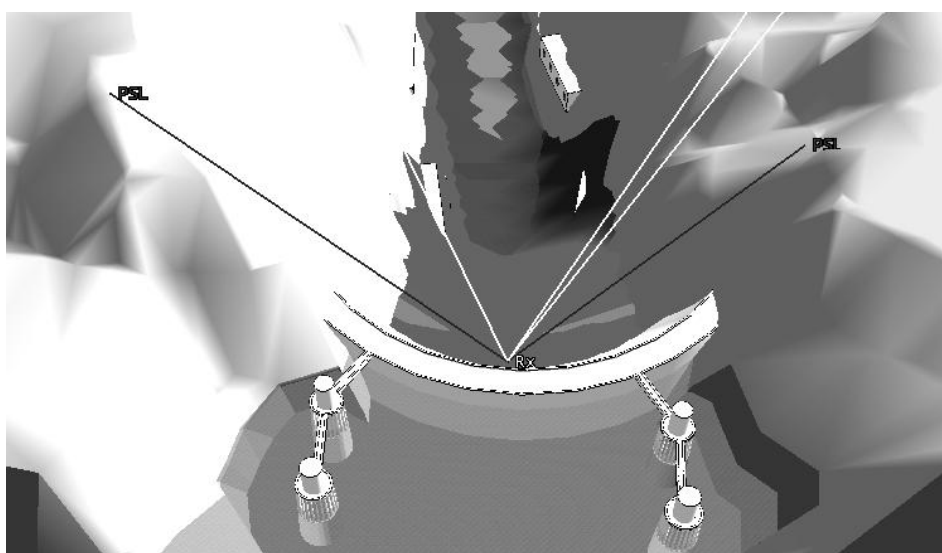


Figure 4 - Hoover dam model. Three visible satellites (grey line), and two pseudolites (black line)

In this paper we demonstrate how augmenting a monitoring system, using only two or three pseudolites, may provide the necessary RTK fixed-integer solutions on a more continuous basis. Furthermore we will assess the overall accuracy improvements when augmenting the system with pseudolites.



4. PSEUDOLITE TO GNSS CARRIER-PHASE DOUBLE DIFFERENCE OBSERVATIONS

In the following we cover the observation equations to be implemented in a typical GNSS-RTK system, based on a combined pseudolite / GNSS satellite signal modelling.

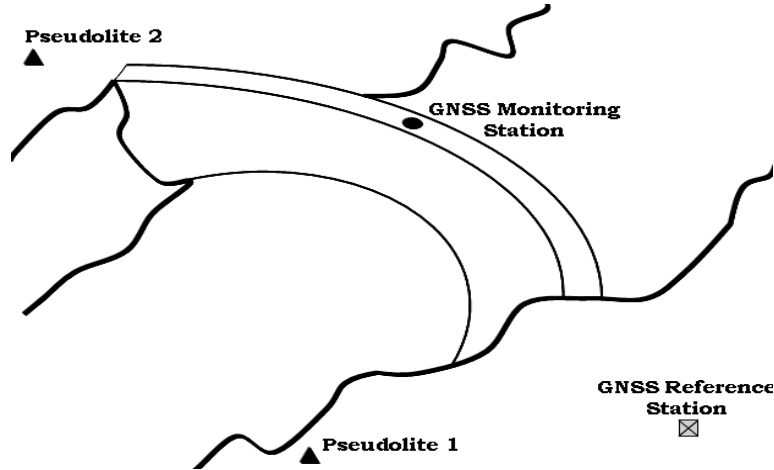


Figure 5 - The relative location of the GNSS stations, and the pseudolite transmitters (not in scale)

The observation equation for the measurements between a satellite and two GNSS receiver stations is given by:

$$\Delta\phi_{m,r}^{prn} = \Delta\rho_{m,r}^{prn} - c\Delta\delta T_{m,r}^{prn} + \Delta\lambda_{L_i} N_{m,r}^{prn} - \Delta I_{m,r}^{prn} + \Delta T_{m,r}^{PRN} + \Delta M_{m,r}^{prn} + \Delta b_{m,r}^{prn} + \Delta\varepsilon_{m,r}^{prn} \quad (1)$$

And for the measurements between a pseudolite and the same two GNSS receiver stations:

$$\Delta\phi_{m,r}^{PSL} = \Delta\rho_{m,r}^{PSL} - c\Delta\delta T_{m,r}^{PSL} + \Delta\lambda_{L_i} N_{m,r}^{PSL} + \Delta\tilde{T}_{m,r}^{PSL} + \Delta\tilde{M}_{m,r}^{PSL} + \Delta\tilde{b}_{m,r}^{PSL} + \Delta\varepsilon_{m,r}^{PSL} \quad (2)$$

Thus one obtains the double-difference pseudolite-to-satellite and master-to-rover observation equation from:

$$\begin{aligned} \Delta\nabla\phi_{m,r}^{PSL,prn} &= \Delta\nabla\rho_{m,r}^{PSL,prn} + \Delta\nabla\lambda_{L_i} N_{m,r}^{PSL,prn} + \Delta\tilde{T}_{m,r}^{PSL} + \Delta\tilde{M}_{m,r}^{PSL} + \Delta\tilde{b}_{m,r}^{PSL} \\ &\quad - \Delta T_{m,r}^{prn} + \Delta I_{m,r}^{prn} - \Delta M_{m,r}^{prn} - \Delta b_{m,r}^{prn} + \Delta\nabla\varepsilon_{m,r}^{PSL,prn} \end{aligned} \quad (3)$$

Where $\Delta\nabla\phi_{m,r}^{PSL,prn}$ is the double-difference carrier-phase measurement between master (m) and rover (r), PSL and prn are the measurements from the pseudolite and satellite, respectively, $\Delta\nabla\rho_{m,r}^{PSL,prn}$ is the double-difference slant-range, $\Delta\nabla\lambda_{L_i} N_{m,r}^{PSL,prn}$ is the double-difference carrier-phase integer ambiguities (λ_{L_i} is the GNSS/pseudolite frequency), $\Delta\tilde{T}_{m,r}^{PSL}$ is the single-difference tropospheric delay from the pseudolite signal (the inverted hat signal represents the special case for pseudolite signals), $\Delta\tilde{M}_{m,r}^{PSL}$ is the single-difference multipath from the pseudolite signal, $\Delta\tilde{b}_{m,r}^{PSL}$ is the baseline error coming from the pseudolite (static) positioning error, $\Delta T_{m,r}^{prn}$, $\Delta I_{m,r}^{prn}$, $\Delta M_{m,r}^{prn}$, $\Delta b_{m,r}^{prn}$ are the usual satellite single-difference carrier-phase tropospheric, ionospheric, and multipath errors, and single-difference satellite orbit error, respectively, and $\Delta\nabla\varepsilon_{m,r}^{PSL,prn}$ is the double-difference carrier-phase system noise.



Pseudolite clocks, $c\Delta\delta_{m,r}^{PSL}$, are of a very low-quality when compared to usual GNSS satellite clocks. Thus in GNSS/Pseudolite-RTK applications it is advisable to use the usual double-difference approach to remove the annoying receiver and emitter clock biases. The terms $\Delta T_{m,r}^{prn}$, $\Delta I_{m,r}^{prn}$, $\Delta b_{m,r}^{prn}$ are properly modelled using usual atmospheric modelling techniques and a short baseline differentiation should remove most of the satellite signal atmospheric and orbit errors. Pseudolite signals are not affected by ionospheric problems as typical pseudolite transmitters are located near the earth's surface. Thus the only atmospheric error remaining will be the pseudolite signal tropospheric delay, that is $\Delta\tilde{T}_{m,r}^{PSL}$.

Standard tropospheric models can not be used to compensate for pseudolite tropospheric delay. This is because model parameters are designed for signals from GNSS satellites, more than 20,000km away [Dai et al., 2001]. Therefore In our simulations we have modelled the troposphere using a simple model, as suggested in the previous reference, where the refractivity n at the base of the atmosphere is described as a function of the meteorological parameters:

$$N = (n - 1) \cdot 10^6 = 77.6(P - e/t) + 71.98(e/t) + 3.75 \cdot 10^5 (e/t^2) \quad (4)$$

Where P is the air pressure in hectopascals, e is the partial pressure of the water vapour in hectopascals, and t is the absolute temperature in degrees Kelvin. If the meteorological parameters can be assumed the same (in normal conditions it should be for distances up to 1,5km) then the term $\Delta\tilde{T}_{m,r}^{PSL}$ is given by:

$$\Delta\tilde{T}_{m,r}^{PSL} = [77.6(P/t) + 5.62(e/t) + 375000(e/t^2)] 10^{-6} \cdot \Delta\rho_{m,r}^{PSL} \quad (5)$$

Unfortunately the term $\Delta M_{m,r}^{prn}$ cannot be easily removed (regardless of the baseline distance). Therefore we will include this term in our simulations using a typical carrier-phase specular multipath reflection model. The same will be done for the respective pseudolite multipath signal $\Delta\tilde{M}_{m,r}^{PSL}$. Due to the pseudolite being static its multipath error ($\Delta M_{m,r}^{PSL}$) is expected to be a nearly constant bias. Consider the forward-scatter problem with a flat specular reflecting lower boundary in Fig. 6 (this is the case of an antenna positioned on top of the dam) where the GNSS antenna is located at point P, at a distance d from the left-hand boundary, height h above the reflecting surface, and with a LOS signal propagating into the domain at angle θ .

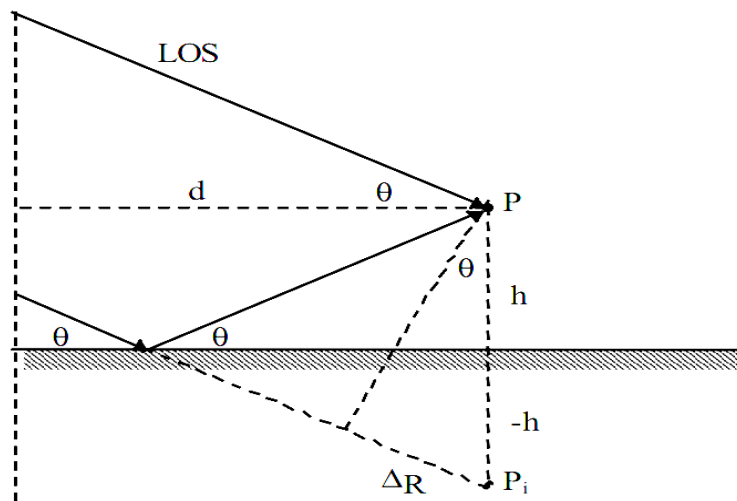


Figure 6 - A 2-D ray-tracing model of forward scatter geometry



In terms of receiver-tracking the main problem is that any additional secondary path will have a time-delay making the reflected signal travel an additional distance ΔR to the image point P_i (always in relation to the LOS point P). This additional path length using basic trigonometric manipulation is given by:

$$\Delta R = 2h \sin \theta \quad (6)$$

The reflection coefficients, derived from the *Fresnel* equations (equations 7 and 8) for a smooth flat surface, provide information on the nature of the reflected signals. GNSS signals are RHCP (Right-Hand Circular Polarized), and circular polarization is the vector sum of the horizontal and vertical polarized waves, that is:

$$\Gamma_H = \left(\sin \theta - \sqrt{\varepsilon - \cos^2 \theta} \right) / \left(\sin \theta + \sqrt{\varepsilon - \cos^2 \theta} \right) \quad (7)$$

$$\Gamma_V = \left(\varepsilon \sin \theta - \sqrt{\varepsilon - \cos^2 \theta} \right) / \left(\varepsilon \sin \theta + \sqrt{\varepsilon - \cos^2 \theta} \right) \quad (8)$$

$$\text{where } \varepsilon = \varepsilon_r - j(\sigma / \omega \varepsilon_0) \quad (9)$$

The reflection coefficient is now estimated for a given frequency, grazing angle θ , dielectric constant and conduction value for the reflecting surface medium [Hannah, 2001]. A plot depicting the reflection coefficient function for a concrete-made specular reflector is given in next figure. The plot represents an effective coupled (Γ_H and Γ_V) reflection coefficient magnitude for an incident L_1 GPS RHCP signal, and for typical antenna attenuation ratios ranging from 0 dB to 30dB.

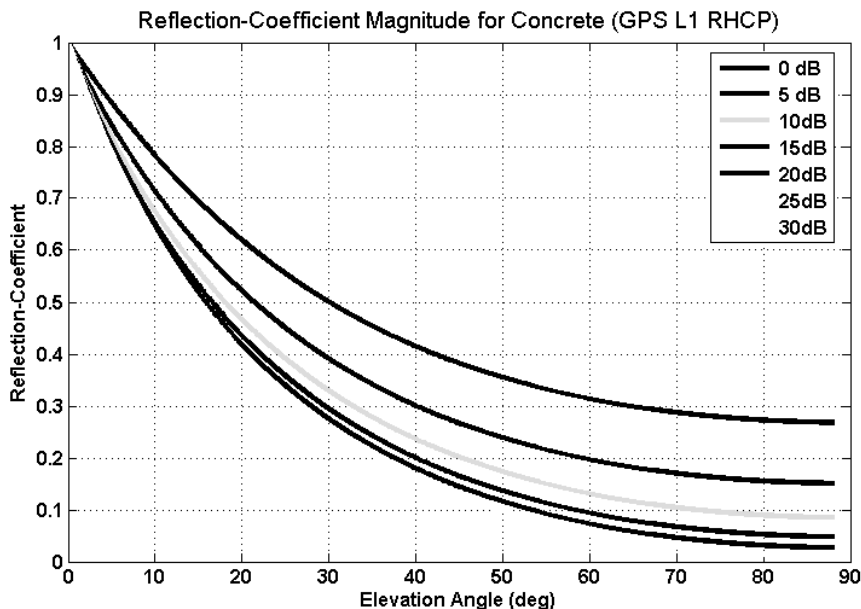


Figure 7 - Concrete reflection coefficient function using several antenna attenuation values.

The results from the carrier-phase multipath software simulation (combining the concrete-based reflection coefficient function, and multipath phase-delay) are given by next figure:

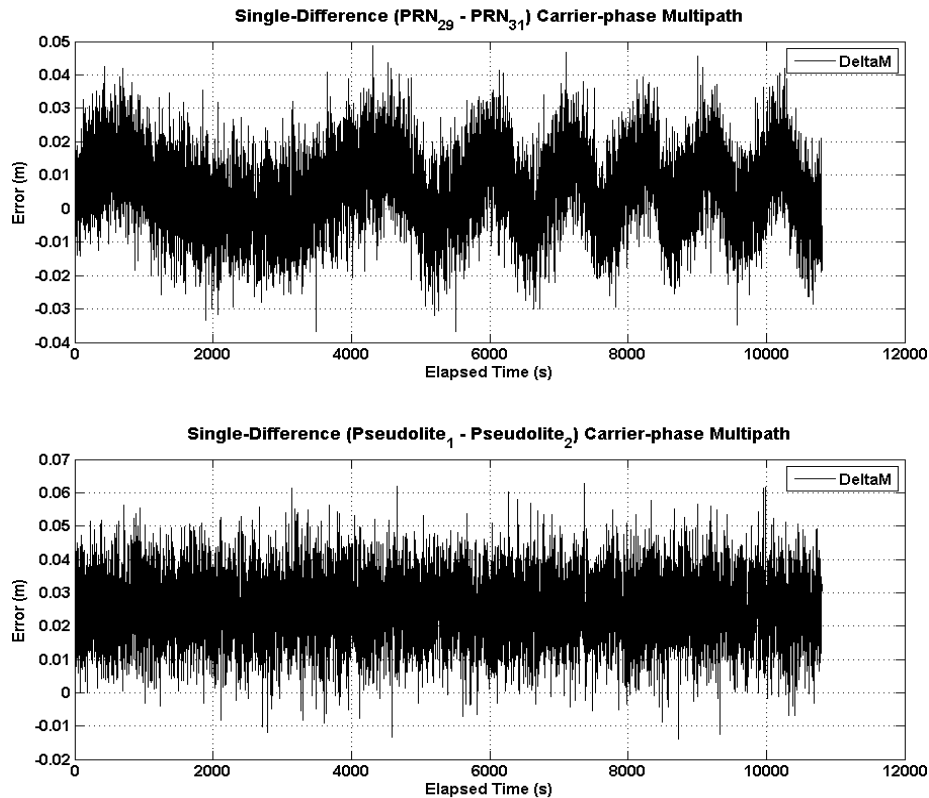


Figure 8 - Single-difference carrier-phase multipath from 2 satellites (top), and from two pseudolites (bottom).

As we can see the single-difference carrier-phase from (static) pseudolite signals is constant in nature and therefore is relatively easy to be estimated in real-time, or calibrated in advance before collecting the data. After obtaining the double-differenced signals generated by our software simulator then we feed it to the GNSS-RTK software. As this is meant to be a monitoring system displacements are expected to affect the monitoring station (on the dam) coordinates. Thus the optimal estimator used is an extended Kalman filter (EKF) where the update (using the transition matrix) of the state parameters is given by:

$$\mathbf{x}_{k+1} = \Phi \mathbf{x}_k \quad \text{and} \quad \mathbf{P}_{x_{k+1}|x_{k+1}} = \Phi \mathbf{P}_{x_k|x_k} \Phi^T + \mathbf{Q}_{ww} \quad (10)$$

Displacements may occur suddenly or slowly-changing in time, and in terms of a position and velocity (PV) system, where the velocity is modelled as a first order Gauss-Markov process, the state update-equation is:

$$\begin{bmatrix} \mathbf{x} \\ \dot{\mathbf{x}} \end{bmatrix}_{k+1} = \begin{bmatrix} 1 & \frac{1 - e^{-\beta \Delta t}}{\beta} \\ 0 & e^{-\beta \Delta t} \end{bmatrix} \begin{bmatrix} \mathbf{x} \\ \dot{\mathbf{x}} \end{bmatrix}_k \quad (11)$$

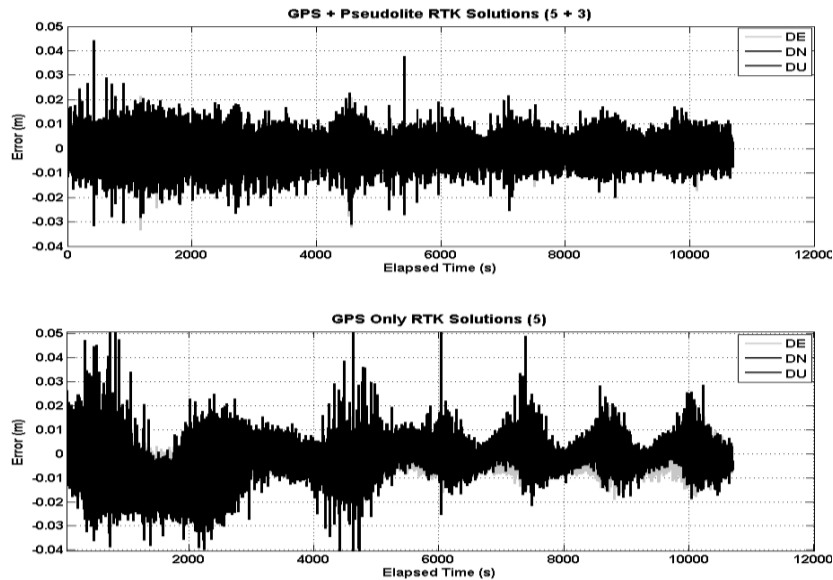


Figure 9 - GPS + Pseudolite-RTK solutions (top), and GPS-only RTK solutions (bottom)

5. TIME SERIES PREDICTION AND DISPLACEMENT DETECTION

The simulation results are given in previous figure. One can see that the inclusion of just two pseudolites is able to remove to a great extent the phase-multipath sinusoidal pattern. It would be difficult in a real-time GNSS-based monitoring system to distinguish a real displacement from typical noisy solutions, especially when outliers occur.

Therefore we implemented a Kalman filter smoother, based on the Rauch-Tung-Striebel (RTS) algorithm (Fig. 10, for up component). A Kalman smoother typically removes most undesirable frequency components from a typical noisy signal. However, when the noise has strong correlations (coloured noise) as the bottom plot then it is rather difficult for the smoothed signal to follow the true signal, that is, the trend caused by the dam displacement.

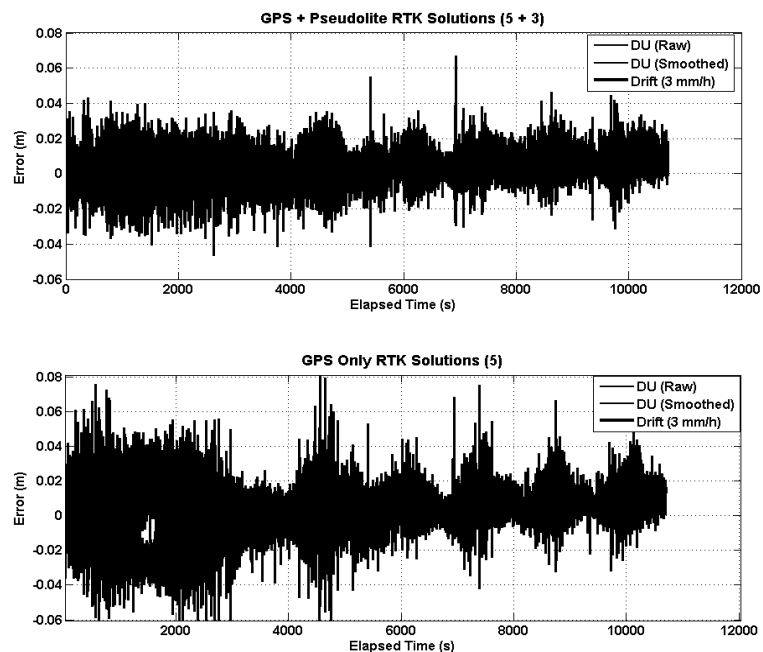


Fig. 10: GPS + Pseudolite smoothed solutions (top), and GPS-only smoothed solutions (bottom)



6. CONCLUSIONS

In this study we have developed a set of simulation tools to evaluate not only the appropriateness (and number) of pseudolite augmentation signals, but as well how they should be employed in an optimal way in order to improve the accuracy and continuity of a typical GNSS-based monitoring system. The RTK coordinates accuracy improvement comparison, depicted in figure 10, is given in next table:

Table 2 - Accuracy comparison of the two signal simulations (GPS-only and GPS+Pseudolite)

	GPS Only RTK Solutions	GPS + Pseudolite RTK Solutions
$RMS_{Easting}$	5mm	4mm
$RMS_{Northing}$	7mm	5mm
RMS_{Up}	9mm	7mm

Moreover the augmentation of only two pseudolite signals allowed the early detection of the simulated slow drift on the Up component. This can be seen in figure 10 where in the top plot the smoother (RTS) algorithm was able to follow accurately the displacement trend, and thus identify at an early stage a potential structural collapse!

On the other hand the bottom picture depicts a problematic scenario where the strong systematic unmodeled biases (coming mostly from carrier-phase multipath reflections from the dam) “mask” the smoothed signal, and do not allow it to evaluate and detect, at least on an early stage, a true displacement trend.

References

Cosser, E., Meng, X., Roberts, G. W., Dodson, A. H., Barnes, J., and Rizos, C. (2004). Precise Engineering Applications of Pseudolites Augmented GNSS, Proceedings of the 1st FIG International Symposium on engineering surveys for Construction Works and Structural Engineering, Nottingham, United Kingdom, June 28-July 1, 2004.

Dai, L., Wang, J., Tsujii, T., and Rizos, C. (2001). Pseudolite applications in positioning and navigation: Modelling and geometric analysis, Proceedings of the International Symposium on Kinematic Systems in Geodesy, Geomatics & Navigation (KIS2001), Banff, Canada, 5-8 June.

Hannah, B. M. (2001). Modelling and Simulation of GPS Multipath, PhD Thesis, The Cooperative Research Centre for Satellite Systems, Queensland University of Technology, Australia, 375 pp.

Serrano, L., D. Kim and R. B. Langley (2008). Carrier-phase multipath calibration in GPS-RTK machine-guidance applications, Proceedings of the IEEE/ION PLANS (Position, Location and Navigation System) 2008, Monterey, California, 5-8 May.

Suh, Y.-C., Konishi, Y., Hakamata, T., and Shibasaki, R. (2002). Development of a Simulation System for Assessing the Layout of Pseudolites in Urban Environment, Proceedings of the 23rd Asian conference on Remote Sensing, Kathmandu, Nepal, November 25-29, 2002.

Contacts

Luis Serrano
 luis.serrano@astrium.eads.net
 EADS Astrium UK Ltd
 United Kingdom